Controlling cluster synchronization by adapting the topology

Judith Lehnert,[1,*] Philipp Hövel,[1,2] Anton Selivanov,[3] Alexander Fradkov,[3,4] and Eckehard Schöll[1]

[1]*Institut für Theoretische Physik, Technische Universität Berlin, Hardenbergstraße 36, 10623 Berlin, Germany*

[2]*Bernstein Center for Computational Neuroscience, Humboldt-Universität zu Berlin, Philippstraße 13, 10115 Berlin, Germany*

[3]*Department of Theoretical Cybernetics, Saint-Petersburg State University, Saint-Petersburg, Russia*

[4]*Institute for Problems of Mechanical Engineering, Russian Academy of Sciences, Bolshoy Avenue, 61, Vasilievsky Ostrov, St. Petersburg, 199178 Russia*

(Received 30 May 2014; published 17 October 2014)

We suggest an adaptive control scheme for the control of in-phase and cluster synchronization in delay-coupled networks. Based on the *speed-gradient method*, our scheme adapts the topology of a network such that the target state is realized. It is robust towards different initial conditions as well as changes in the coupling parameters. The emerging topology is characterized by a delicate interplay of excitatory and inhibitory links leading to the stabilization of the desired cluster state. As a crucial parameter determining this interplay we identify the delay time. Furthermore, we show how to construct networks such that they exhibit not only a given cluster state but also with a given oscillation frequency. We apply our method to coupled Stuart-Landau oscillators, a paradigmatic normal form that naturally arises in an expansion of systems close to a Hopf bifurcation. The successful and robust control of this generic model opens up possible applications in a wide range of systems in physics, chemistry, technology, and life science.

DOI: 10.1103/PhysRevE.90.042914 PACS number(s): 05.45.Xt, 87.85.dq, 89.75.−k

I. INTRODUCTION

Networks play a prominent role in the research of very different fields, ranging from social science, economics, and psychology to biology, physics, and mathematics [1–3], as they are a straightforward concept to describe the interactions of many systems or agents. While previous research focused either on the formation of topologies [1–6] or on the dynamics on a network with fixed topology [7–15], adaptive networks bring these two aspects together: In such networks the topology evolves according to the state of the system while the dynamics on the network and thus the state is influenced by the topology [16].

Among the variety of well-studied dynamical scenarios, in-phase synchronization has been the main focus of research concerning the dynamics on networks for a long time. Recently, more complex synchronization patterns, including cluster and group synchronization have received growing interest both in theory [11,17–21] and in experiments [22,23]. These scenarios appear in many biological systems; examples include dynamics of nephrons [24], central pattern generation in animal locomotion [25], or population dynamics [26]. In an M-cluster state, for instance, the compound system evolves to M clusters with in-phase synchronization between the nodes of one cluster and—in the case of an oscillatory system—with a constant phase lag of $2\pi/M$ between the clusters. In contrast, group synchronization refers to the case where each cluster potentially exhibits different local dynamics.

Control of cluster synchronization by adaptively changing the topology of the network has previously been investigated, to our knowledge, by only a few researchers: Lu and Qin consider control of cluster synchronization by means of changing topology. As a limiting restriction for its applicability, their method requires *a priori* knowledge of to which cluster each node should belong in the final state [27]. Furthermore, the majority of algorithms developed to control (mainly in-phase) synchronization by adaptation of the network topology are based on local mechanisms. Most of them are related to Hebb's rule: *Cells that fire together, wire together* [28]. Our method uses a global goal function to realize self-organized control and is therefore a powerful alternative and complements existing control schemes.

In Ref. [29], the control of cluster synchronization by adapting the phase of a complex coupling strength was shown. While this method is an easy and elegant way to control small networks by tuning of just one parameter, it fails for larger networks because it becomes too sensitive to initial conditions.

Here, we present an algorithm to adapt the topology of a network in such a way that a desired cluster state is reached. The method is not only robust towards initial conditions but also works for a large parameter range. The adaption algorithm for the network structure employs the *speed-gradient method* [30]. As a strong advantage compared to other methods, no *a priori* ordering of nodes is needed, i.e., it is not necessary to assign each node to a specific cluster in advance. In contrast, the final assignment is a built-in consequence of the initially designed goal function.

Aiming for a general framework, we consider the Stuart-Landau oscillator, which is the normal form of a Hopf bifurcation and therefore generic for many oscillating systems present in nature and technological applications. In addition, we implement time-delayed coupling between the nodes because delays naturally arise in many applications. Note that our scheme also works for instantaneous coupling.

Furthermore, it is not necessary to control all links of a network. The control scheme remains successful if only a subset of links is accessible. We will explicitly demonstrate this by applying the method to parts of a random network [31], while retaining control of the target state.

To what extent structure determines function, i.e., which topologies allow for cluster synchronization, is a hot topic

*Corresponding author: lehnert@itp.tu-berlin.de

of current research [18–20]. Our method provides an easy and self-organized way to generate weighted networks that are able to exhibit cluster synchronization. The topology of these networks will contain some randomness as we start with random initial conditions for the state of the node. However, on average the topology is characterized by common features that enable synchronization and hence yield the desired cluster state. As a crucial parameter shaping this topology we identify the delay time. Furthermore, we show how to construct networks in which cluster states oscillate with a desired frequency (including zero frequency).

In the following section, we describe the model and establish the target states. Section III discusses the goal function and briefly reviews the speed-gradient method. The central part of the paper is Sec. IV, in which the adaption algorithm for the topology is developed and demonstrated. The structure of the networks after successful control is discussed in Sec. V, where we also show how a discrete Fourier transform of the coupling matrix can be used to get insight into the delay-modulated topology. Section VI shows how the obtained results can be used not only to control cluster synchronization, but also to grow networks in which a cluster state with a given frequency is stable. We conclude with Sec. VIII.

II. MODEL

The system equation of a Stuart-Landau oscillator is given by

$$\dot{z} = [\lambda + i\omega - |z|^2]z, \tag{1}$$

with the complex variable $z \in \mathbb{C}$ and $\lambda, \omega \in \mathbb{R}$ [32]. It arises in a center manifold expansion close to a supercritical Hopf bifurcation with λ as the bifurcation parameter. For $\lambda < 0$, the system exhibits a stable focus. At the bifurcation point $\lambda = 0$, the focus loses stability, and a stable limit cycle with radius $\sqrt{\lambda}$ is created. The parameter ω denotes the frequency of the uncoupled node.

In the following, we consider a system of N delay-coupled Stuart-Landau oscillators z_j, $j = 1, \ldots, N$:

$$\dot{z}_j(t) = [\lambda + i\omega - |z_j|^2]z_j + K\sum_{n=1}^{N} G_{jn}(t)[z_n(t-\tau) - z_j(t)], \tag{2}$$

where K is the overall coupling strength, and τ is the delay time. In the following, we denote delayed variables by an index τ, e.g., $z_\tau \equiv z(t-\tau)$. $\{G_{jn}(t)\}_{j,n=1,\ldots,N}$ is the coupling matrix describing the topology of the network and subject to the adaptive control.

Equation (2) can be rewritten in amplitude and phase variables with $r_j = |z_j|$ and $\varphi_j = \arg(z_j)$:

$$\begin{aligned} \dot{r}_j(t) &= \left[\lambda - r_j^2\right] r_j + K\sum_{n=1}^{N} G_{jn}\{r_{n,\tau}\cos[\varphi_{n,\tau} - \varphi_j] - r_j\}, \\ \dot{\varphi}_j(t) &= \omega + K\sum_{n=1}^{N} G_{jn}\left\{\frac{r_{n,\tau}}{r_j}\sin[\varphi_{n,\tau} - \varphi_j]\right\}. \end{aligned} \tag{3}$$

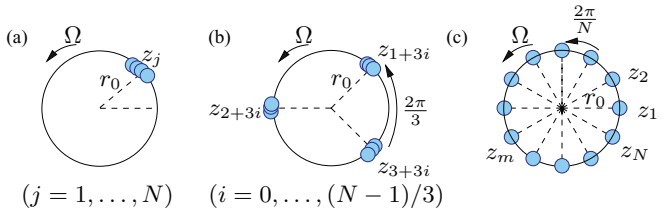

FIG. 1. (Color online) Schematic view of (a) in-phase synchronization ($M = 1$), (b) a three-cluster ($M = 3$), and (c) a splay state ($M = N$). Each cluster consists of the same number of nodes.

Cluster states are possible solutions of Eq. (3). They exhibit a common amplitude $r_j \equiv r_0$ and phases given by $\varphi_j = \Omega_m t + j2\pi/M$, where Ω is the collective frequency. The integer M determines the number of clusters. Here, we assume that M is a factor of N. Special cluster states are in-phase (also called zero-lag) synchronization ($M = 1$), where all nodes are in one cluster, and the splay state ($M = N$), where each cluster consists of a single node. In the continuum limit, the splay state on a unidirectionally coupled ring corresponds to a rotating wave. For a schematic diagram of (a) in-phase synchronization, (b) a three-cluster state, and (c) a splay state see Fig. 1.

The stability of synchronized oscillations in networks can be determined numerically, for instance, by the *master stability function* [33]. This formalism allows for a separation of the local dynamics of the individual nodes from the network topology. In the case of the Stuart-Landau oscillators it is possible to obtain the Floquet exponents of different cluster states analytically with this technique [9]. By these means it has been demonstrated that the unidirectional ring configuration, i.e., $G_{ij} = \delta_{(i+1) \bmod N, j}$, of Stuart-Landau oscillators exhibits multistability between in-phase synchrony, splay states, and clustering in a large parameter range. The main goal of the adaptive topology developed here is to suppress the multistability and to stabilize the desired cluster state even for parameters for which it would be unstable in the unidirectional ring. To find an appropriate adaptive control, we make use of the speed-gradient method [30], which is outlined in the next section.

Note that in theory synchronized states could coexist where the phase lags between different clusters are of unequal size [22]. Such a phenomenon is called phase multistability and could be an additional challenge to our control method. However, such states have not been observed in the Stuart-Landau oscillator probably because of the sinusoidal form of its oscillations. Furthermore, our goal function (see the next section) is designed such that it has in general only a minimum for the desired cluster states and thus would prefer this state over states with unequal phase lags.

III. SPEED-GRADIENT METHOD AND GOAL FUNCTION

The main ingredient of the speed-gradient method [30] is a goal function $Q(z(t),t)$ that has a minimum (often equal to zero) in the target state, i.e., a state consisting of M equally sized clusters with a constant phase lag between subsequent clusters, and larger than this minimum otherwise.

An appropriate goal function $\tilde{Q}_M$ to control an M-cluster state was suggested in Refs. [29,34]:

$$\tilde{Q}_M = 1 - f_M(\varphi) + \frac{N^2}{2} \sum_{p|M, 1\leqslant p<M} f_p(\varphi), \tag{4}$$

where $p|M$ denotes that p is a factor of M. The function $f_M(\varphi) = \frac{1}{N^2} \sum_{j=1}^{N} e^{iM\varphi_j} \sum_{k=1}^{N} e^{-iM\varphi_k}$, where φ_j is the phase of the jth oscillator, $j = 1,\ldots,N$, and $\varphi \equiv (\varphi_1,\ldots,\varphi_N)$ is a generalization of the Kuramoto order parameter [32] and approaches unity for an M-cluster state. Since $f_M = 1$ holds not only in the desired M-cluster state, but also for all divisors p of M, a goal function of the form $\tilde{Q}_M = 1 - f_M(\varphi)$ would also vanish if the system were in one of the p-states. Therefore, the term $\sum_{p|M,1\leqslant p<M} f_p(\varphi)$ in Eq. (4) was added as a penalty term.

Equation (4) can be used to control cluster synchronization by means of adapting the topology and, in fact, the results are qualitatively similar to the ones presented in this paper. However, Eq. (4) has two drawbacks: First, it only ensures phase synchronization, i.e., the radii of the oscillators do not synchronize, and, second, the clusters are not of equal size. Therefore, we use an extended version of Eq. (4):

$$Q_M = \underbrace{1 - f_M(\varphi) + \frac{N^2}{2} \sum_{1\leqslant p<M} f_p(\varphi) + \frac{1}{2} \sum_{i,k=1}^{N} (r_i - r_k)^2}_{q_M} + \frac{c}{2} \int_0^t \sum_{k=1}^{N} \left(\sum_{i=1}^{N} G_{ki}(t') - 1 \right)^2 dt'. \tag{5}$$

We drop the condition $p|M$, in other words we add penalty terms for all p-cluster states, where $p < M$. This ensures clusters of equal size since it prevents side maxima of the goal function. Synchronization of the radii is reached due to the term $\sum_{i,k}(r_i - r_k)^2$, where r_i is the amplitude of the ith oscillator. The last term in Eq. (5), where (G_{ki}) is the $N \times N$ coupling matrix and $c > 0$ is a parameter, yields a unity row sum. Without it, a constant but arbitrary row sum would arise. Ensuring unity row sum helps to avoid side effects of changing the effective coupling strengths by this arbitrary row sum. As this term takes into account all deviations from the unity row sum during the growth of the network, Q_M will not vanish completely in the goal state. Thus, q_M is a better measure for the quality of synchronization. Though this might be regarded as a disadvantage of the integral in the unity-row-sum term, the advantage of the integral is that only terms in G_{ij} but not in $\dot{G}_{ij}$ appear in the right-hand side of the speed-gradient algorithm. Thus, it is not necessary to solve for $\dot{G}_{ij}$.

The speed-gradient method [30] is generally used in the control of nonlinear systems of the form $\dot{z} = F(z,u,t)$, where $z \in \mathbb{C}^n$ is the state vector, $u \in \mathbb{C}^m$ is an input (control) variable, and F is a nonlinear function. The speed (or rate) at which $Q(z(t),t)$ is changing along the trajectory of $z(t,u)$ is given by $v(z,u,t) = \dot{Q} = \partial Q(z(t),t)/\partial t + [\nabla_z Q(z(t),t)]^T F(z,u,t)$. The idea of the speed-gradient method is to change the control u in the direction of the negative gradient of $v(z,u,t)$ with respect to the input variables:

$$\frac{du}{dt} = -\gamma \nabla_u v(z,u,t), \tag{6}$$

where γ is a positive definite gain matrix. The intuition behind the speed-gradient method is that $\dot{Q}$ may decrease along the direction of its negative gradient and as $\dot{Q}$ becomes negative, Q will decrease as well and may finally tend to the minimum, i.e., the control goal is reached. In fact those statements hold under some additional conditions [35,36].

IV. ADAPTING THE TOPOLOGY

Using Eq. (6) with $u = (G_{11},G_{12},\ldots,G_{N,N-1},G_{NN}) \in \mathbb{R}^{N^2}$ and $\gamma_{ij} = \delta_{ij}\gamma_G$, where γ_G is a positive constant, we obtain the following control scheme:

$$\dot{G}_{jn}(t) = -\gamma_G K \left[\frac{r_{n,\tau}}{r_j} \sin(\varphi_{n,\tau} - \varphi_j) \right] \times \sum_{k=1}^{N} \left\{ \sum_{1\leqslant p<M} p \sin[p(\varphi_k - \varphi_j)] - \frac{2M}{N^2} \sin[M(\varphi_k - \varphi_j)] \right\} - 2\gamma_G K \sum_{k=1}^{N} (r_j - r_k) \left[r_{n,\tau} \cos(\varphi_{n,\tau} - \varphi_j) - r_j \right] - \gamma_G c \left(\sum_{i=1}^{N} G_{ji} - 1 \right). \tag{7}$$

Figure 2 shows an example of the evolution of the network by applying the control algorithm (7) with Q_8, i.e., the goal of reaching an eight-cluster state. The initial topology is a unidirectional ring; see Fig. 2(a). However, the nodes are approximately depicted according to their position z_j in the phase space; because these phase differences are initially random, the unidirectional coupling structure does not clearly show here. At $t = 0$ the control is switched on [Fig. 2(b)], and links change rapidly as can be seen in Fig. 2(c). The final state of the network is shown Fig. 2(d): eight equally sized clusters are formed (to distinguish all nodes, the nodes in one cluster are not depicted exactly according to their phases but on a circle around the point which would correspond to their phase and radius). Black links mark excitatory links, i.e., links that correspond to positive entries of the coupling matrix, while the gray (light blue) links are inhibitory ones, i.e., links due to negative entries of the coupling matrix. Clearly, the final topology is characterized by a distinct distribution of excitatory and inhibitory links: While the inhibitory links mainly connect neighboring clusters, the excitatory ones dominate the connections to clusters further away in phase space. In the next section this distribution is investigated more closely.

Corresponding to the network realization in Fig. 2, Fig. 3 shows the time series of (a) the radii, (b) the phase differences, (c) the coupling weights, and (d) the goal function. After the

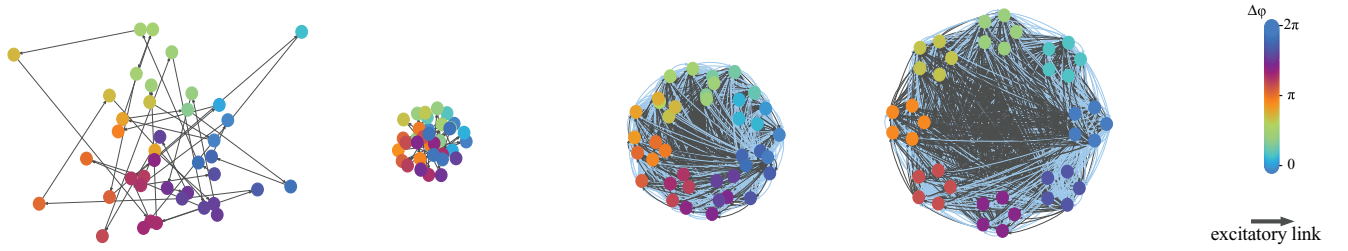

(a) $t = -50$ (initial state) (b) $t = 0$ (control starts) (c) $t = 2$ (shortly after control started) (d) $t = 50$ (final state)

FIG. 2. (Color online) Evolution of the network topology with the goal to achieve an eight-cluster state. Black, excitatory weighted links; gray (blue), inhibitory weighted links. Node colors denote phase differences with respect to the first node. Parameters: $\lambda = 0.1, \omega = 1, c = 0.01, K = 0.1, \tau = \pi, \gamma_G = 10, N = 40, M = 8$.

control is switched on, the radii and phases rapidly converge to the eight-cluster state, and Q_8 and q_8 approach their minimum.

V. STRUCTURAL PROPERTIES

In the field of complex networks, topological features that enhance or weaken synchronizability are of great interest [10,14,15,33]. Here, we discuss the structural properties of the networks after successful control, in order to elucidate the common features that enable synchronization in a cluster state. To do so we consider the coupling weights of the final topology as a function of the final phase difference, i.e., the function $\tilde{G}_{ij}(\Delta_{ij})$ where $\Delta_{ij} \equiv \lim_{t\to\infty}[\varphi_i(t) - \varphi_j(t)]$. In Fig. 4 we plot

$$\bar{G}\left(\frac{2\pi}{M}n\right) = \left\langle \sum_{\substack{ij \\ (\Delta_{ij}) \in I_n}} G_{ij}(\Delta_{ij}) \right\rangle \tag{8}$$

with the interval $I_n = (\frac{2\pi n - \pi}{M}, \frac{2\pi n + \pi}{M}]$, where $n = -M/2, \ldots, M/2 - 1$ if M is even and $n = -(M-1)/2, \ldots, (M-1)/2$ if M is odd. $\langle\cdot\rangle$ denotes the ensemble average over 100 realizations, i.e., $\bar{G}(\frac{2\pi}{M}n)$ is the average of all weights linking nodes which have a phase difference in the interval I_n. In the case of successful control these are the weights linking nodes in cluster i with nodes in cluster $(i + n)$ mod M. Figure 4 depicts the weights for different delay times. Obviously, the curves have the form of a time-shifted cosine, i.e., $\bar{G}(\frac{2\pi}{M}n) \propto \cos(\frac{2\pi n}{M} - \tau)$. This explains the topological structure we observe in Fig. 2(c): Since $\tau = \pi$, we expect a structure as described by Fig. 4(c). Thus, a negative coupling between nodes with a small phase difference and a positive coupling between nodes with a phase equal or close to π.

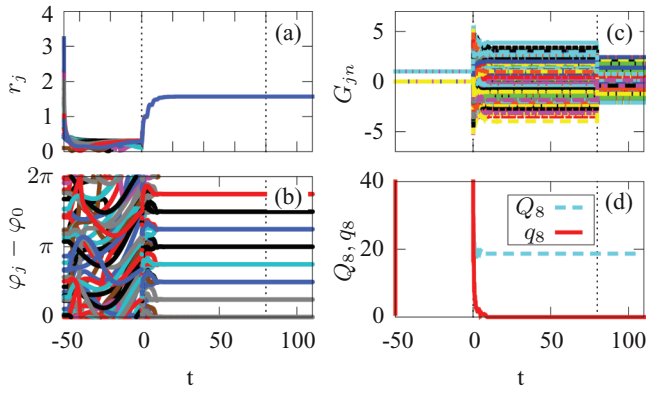

FIG. 3. (Color online) Control of an eight-cluster state: (a) radii r_j, (b) phase difference $\varphi_j - \varphi_0$ with respect to the first node, (c) coupling weights G_{ij}, and (d) goal function Q_8 [dashed gray (turquoise) line] and its reduced part q_8 (black (red) line) which excludes the unity-row-sum term. Control starts at $t = 0$. The vertical dotted line at $t = 80$ is explained in Sec. V B. Parameters as in Fig. 2.

A. Existence of cluster solutions

Insight into the network structure can be obtained by a row-wise discrete Fourier transform of the coupling matrix after successful control. To do so, we introduce the following $N \times M$ matrix:

$$\Gamma_{jk} = \sum_{l=0}^{m-1} \tilde{G}_{j,k+lM}, \tag{9}$$

where m is the number of nodes in one cluster, i.e., $m = N/M$, and the tilde denotes the final topology of the network, i.e., $\tilde{G} = G(t_\infty)$. Here, we label the nodes such that the

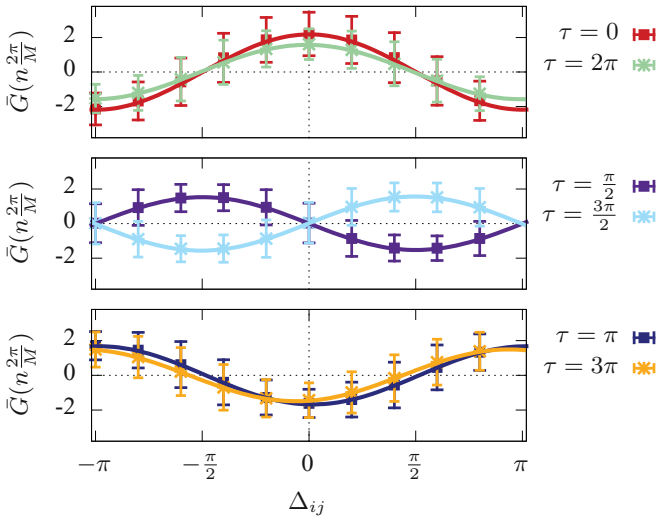

FIG. 4. (Color online) Average link strength $\bar{G}(\frac{2\pi}{M}n)$ versus phase differences $\Delta_{ij} = \lim_{t\to\infty}[\varphi_i(t) - \varphi_j(t)]$ in the final state as defined in Eq. (8). $N = 30$, $M = 10$. Average over 100 realizations. Other parameters as in Fig. 2.

synchronized state can be described by

$$r_j \equiv r_0, \quad \varphi_j \equiv \Omega t + j\frac{2\pi}{M}, \tag{10}$$

for $j = 1, \ldots, N$, where r_0 and Ω denote the common radius and the common frequency, respectively. Thus, Γ_{jn} represents the total input which node j receives from all nodes in cluster n. We now represent each row of Γ as a discrete Fourier series

$$\Gamma_{jk} = \frac{b_0^j}{2\cos(\Omega\tau)} + \sum_{l=1}^{N_0-1} a_l^j \sin(\Phi_{l,k,j}) + b_l^j \cos(\Phi_{l,k,j}) + \underbrace{\frac{b_{N_0}^j}{\cos(\Omega\tau)^2}\cos\left(\Phi_{N_0,k,j}\right)}_{\text{if } M \text{ is even}} \tag{11}$$

with the abbreviation $\Phi_{l,k,j} = l(k-j)2\pi/M - \Omega\tau$. $N_0 = (M+1)/2$ if M is odd and $N_0 = M/2$ if M is even. The coefficients are given by

$$\begin{aligned} a_l^j &= \frac{2}{M}\sum_{k=1}^{M}\Gamma_{jk}\sin(\Phi_{l,k,j}) = \frac{2}{N}\sum_{k=1}^{N}\tilde{G}_{jk}\sin(\Phi_{l,k,j}) \\ b_l^j &= \frac{2}{M}\sum_{k=1}^{M}\Gamma_{jk}\cos(\Phi_{l,k,j}) = \frac{2}{N}\sum_{k=1}^{N}\tilde{G}_{jk}\cos(\Phi_{l,k,j}). \end{aligned} \tag{12}$$

From the constant row sum condition, i.e., $\sum_{k=1}^{M}\Gamma_{jk} = \sum_{k=1}^{N} G_{jk} = 1$, $b_0^j = \frac{1}{2M\cos(\Omega\tau)}$ follows. $\bar{G}(\frac{2\pi}{M}n)$ can be expressed as $\bar{G}(\frac{2\pi}{M}n) = \langle\sum_{j=1}^{N}\Gamma_{j,(j+n) \bmod M}\rangle$.

Next, we discuss the necessary condition for a_l^j and b_l^j such that an M-cluster state exists as a solution of Eq. (3). Substituting Eq. (10) into Eq. (3) yields the following conditions for r_0 and Ω:

$$\begin{aligned} r_0^2 &= \lambda + K\sum_{k=1}^{N}\tilde{G}_{jk}\left[\cos(\Phi_{1,k,j}) - 1\right], \\ \Omega &= \omega + K\sum_{k=1}^{N}\tilde{G}_{jk}\sin(\Phi_{1,k,j}). \end{aligned} \tag{13}$$

Using Eq. (12) this can be rewritten as

$$r_0^2 = \lambda + K\left[\frac{b_1^j N}{2} - 1\right], \tag{14a}$$

$$\Omega = \omega + K\left[\frac{a_1^j N}{2}\right]. \tag{14b}$$

Equation (14) has to be fulfilled for all $j = 1, \ldots, N$. Thus, only if $a_1^1 = a_1^2 = \cdots = a_1^N \equiv a$ and $b_1^1 = b_1^2 = \cdots = b_1^N \equiv b$ does a solution with a common radius and a common frequency exist. Note that there is no restriction on the higher Fourier coefficients, i.e., on a_l^j and b_l^j with $l > 1$.

B. Stability of cluster states

So far we have discussed the existence of the solution, but not its stability. Unfortunately, it is not possible to carry out a systematic stability analysis in all Fourier coefficients as their number is too high for large M. However, there is evidence that the higher Fourier coefficients do not affect the stability. Figure 5 shows the b_l^j, $j = 1, \ldots, N$, $l = 1, \ldots, N_0$ corresponding to the simulation shown in Fig. 3. Clearly, the b_1^j converge to a common value b after the control has been switched on at $t = 0$ assuring the existence of a common radius according to Eq. (14). In contrast, the higher Fourier coefficients do not approach each other. At $t = 80$, we set each of the higher Fourier coefficients to a random value in the interval $[-3,3]$.[1] As expected and apparent in Figs. 3 and 5, a and b, and thus the common frequency and radius, do not change as a result of this perturbation. The higher Fourier coefficients stay at their new values, since there is no need for them to readjust. In conclusion, the existence and stability of the cluster solution do not depend on the higher Fourier coefficients. Thus, the final values of these higher coefficients follow from the random initial conditions and are therefore random themselves. As a consequence they average out, while, on average, the first Fourier coefficients dominate the topology. In fact, the average topology is mainly given by b as a and $b_0 = \frac{1}{N}$ are typically small. Thus, $\bar{G}(\frac{2\pi}{M}n) = \langle\sum_{j=1}^{N}\Gamma_{j,(j+n) \bmod M}\rangle \approx b\cos(\frac{2\pi}{M}n - \Omega\tau)$ explaining the cosine form of the curves shown in Fig. 4.

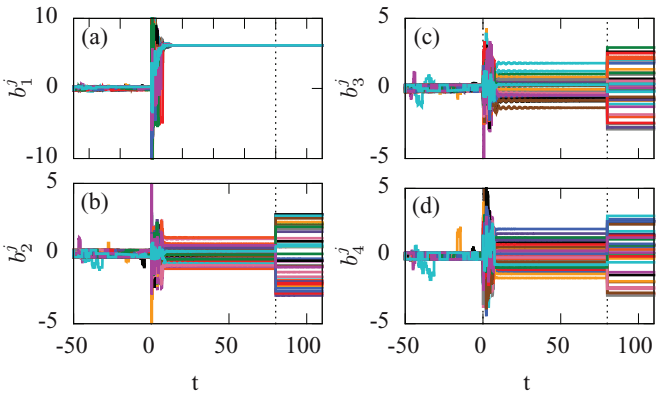

FIG. 5. (Color online) Control of an eight-cluster state: Fourier coefficients as defined in Eq. (12): (a) b_1^j, (b) b_2^j, (c) b_3^j, and (d) b_4^j. At $t = 80$, b_2^j, b_3^j, and b_4^j are set to random values. Parameters as in Fig. 2.

VI. CHOOSING A FREQUENCY

The representation of the coupling matrix in a Fourier series as in Eq. (11) is particularly convenient if one wants to choose a common frequency via constructing an appropriate matrix. To select the common frequency Ω_0, we set $a = \frac{2}{N}(\frac{\Omega_0-\omega}{K})$ according to Eq. (14b). As an example, we show in Fig. 6 the quenching of oscillations in a splay state, i.e., we tune the common frequency Ω_0 of all nodes to zero, which corresponds to a stationary state: At $t = 0$ we start the adaptive control with $M = N$, i.e., with the goal function leading to a splay state. At $t = 40$ the adaptive control is switched off and a is kept

[1] We chose this interval for convenience of depiction. Qualitatively, the result is the same for much larger random numbers.

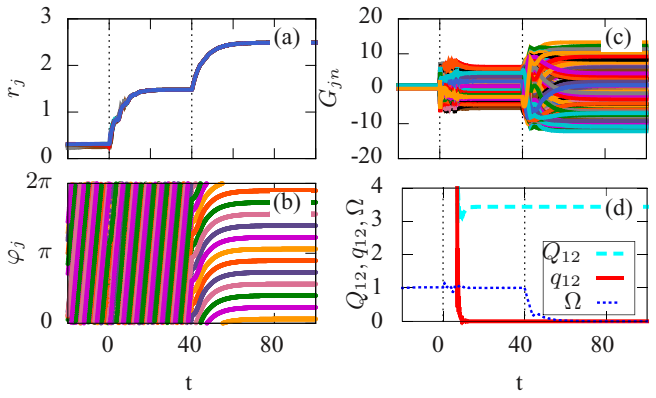

FIG. 6. (Color online) Oscillation quenching of a splay state: (a) radii r_j, (b) phases φ_j, (c) coupling weights G_{ij}, and (d) goal function Q_{12} [black (red) line], its reduced part q_{12} [gray (turquoise) line], and the collective frequency Ω [black (blue) dotted line]. $N = 12$, $M = 12$. At $t = 40$ the adaptive control is switched off and a is set to $a = \frac{2\omega}{NK}$. Other parameters as in Fig. 2.

fixed at $a = \frac{2\omega}{NK}$ forcing Ω to approach zero. As a result of Ω_0 decaying to zero while a is fixed, the coupling weights slightly change after $t = 40$ even though the adaptive control is switched off.

VII. CONTROL OF A SUBSET OF LINKS

So far we have controlled every link of the network. However, this is not necessary. It is sufficient to control a subset of links, while the other links are left fixed. We demonstrate this with an example of a directed random network constructed of P links, which are chosen from the $L = N(N-1)$ possible links excluding self-coupling. From these P links, we select, again randomly, A links which are subject to adaptation as given by Eq. (7). As an example, Fig. 7 depicts the generation of a three-cluster state in a network of 15 notes. Figure 7(a) shows the network before the control: Black links mark the $P - A$ fixed links; gray (green) links depict the A links that will be adapted. Obviously, only these links change their strength during the adaptation process as can be seen in Fig. 7(b), which displays the network after it has reached the desired three-cluster state and the change of topology terminates.

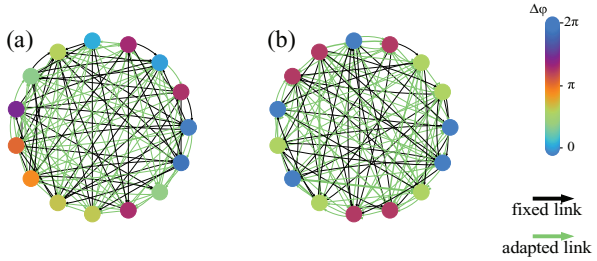

FIG. 7. (Color online) Topology (a) before ($t = 0$) and (b) after control ($t = t_c$). Black links, fixed links; gray (green), adapted links. Color code of nodes, phase difference $\Delta\varphi = \varphi_j - \varphi_0$ with respect to the first node. Parameters: $\tau = 3$, $A/L = 0.3$, $P/L = 0.4$, $N = 15$, $M = 3$. Other parameters as in Fig. 2. Initial conditions: directed random network.

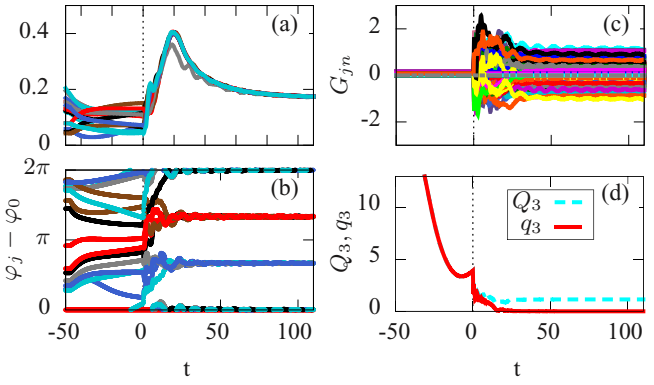

FIG. 8. (Color online) Restricted control of a three-cluster state: (a) radii r_j, (b) phase difference $\varphi_j - \varphi_0$ with respect to the first node, (c) coupling weights G_{ij}, and (d) goal function Q_3 [gray (turquoise) dashed line] and it its reduced part q_3 [black (red) line]. Parameters as in Fig. 7.

The corresponding time series are shown in Figs. 8(a)–8(d) for the radii, the phase differences, the elements of the coupling matrix, and the goal function, respectively. As can be seen in Figs. 8(b) and 8(d), after successful control with goal function Q_3 the network consists of three equally sized clusters and the reduced goal function q_3 is zero.

We now want to test how successful our method is in dependence upon the links present in the networks, and upon the fraction of these links subject to adaptation: Figure 9 shows the fraction f_c of successfully controlled networks and as an inset, the control time t_c as a function of P/L and A/L. We define a network as successfully controlled in an M-cluster state (including the cases of unequally sized clusters just discussed) at time t_c if it was in this state for $t \in [t_c - 1, t_c]$.

Note that the success rate is fairly independent of the total number of links P in the network, but depends mainly on the ratio of adapted links to all possible links. In other words, the links additionally present in the network, but not subject to

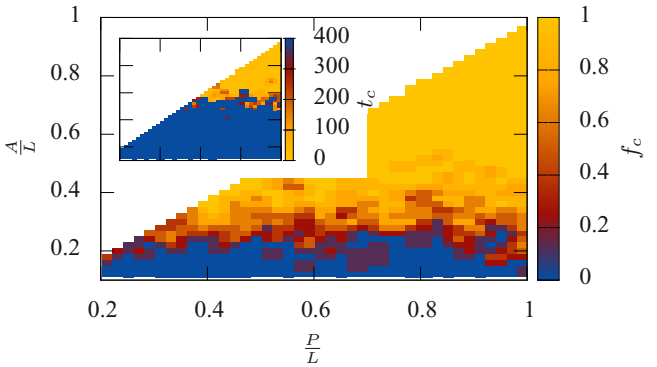

FIG. 9. (Color online) Fraction f_c of successfully controlled networks as a function of number of random links P and number of controlled links A, normalized by $L = N(N-1)$. Inset: times t_c needed to reach the control goal. $K = 0.2$. We simulated ten realizations for each parameter combination. Other parameters as in Fig. 7.

control, have almost no effect on the synchronizability. If the number of adapted links reaches about 30% the control still works in more than 80% of the cases.

Furthermore, we study f_c and t_c in dependence on the coupling strength K and the delay time τ for a fully connected and adapted network, i.e., $P/L = A/L = 1$. We find that the fraction of successfully controlled networks f_c is close to 1 and t_c is roughly 10 units in the considered range $0.1 < K \leqslant 5$, $0 \leqslant \tau \leqslant 3\pi$ (not shown here), demonstrating that our method works very reliably independently of the coupling parameters.

VIII. CONCLUSION

We have proposed a method to control cluster synchronization in a network of time-delay coupled oscillators. Our method uses the speed-gradient algorithm to adapt the topology. The considered goal function is based on a generalized Kuramoto order parameter and is independent of the ordering of the nodes. An additional term ensures amplitude synchronization. The control scheme is very robust. Numerically, we studied the robustness towards different initial conditions and its dependence on the overall coupling strength and delay time.

The topology of the network after successful control is modulated by the coupling delay. A row-wise discrete Fourier transform of the coupling matrix gives insight into these delay modulations. Necessary conditions for the existence of a common radius and a common frequency give rise to restrictions affecting the first Fourier coefficients, while there is no restriction for the higher Fourier coefficients. We also found that the stability of the cluster states is not affected by the higher Fourier coefficients. Thus, we conclude that the higher Fourier coefficients are mainly dependent on the random initial conditions and are therefore randomly distributed. On average, the network topology is therefore dominated by the first Fourier coefficients leading to the observed delay modulation.

We show that we can make use of the first Fourier coefficients in order to find topologies that lead to cluster states with a given common frequency. As an example, we quench the oscillations in a Stuart-Landau oscillator. Thus, we have found a very versatile method to construct networks which show a desired dynamical behavior.

Since in many real-world networks not all links are accessible to control, we applied the adaptation algorithm to random networks where we chose a random subset of links which we controlled, while the other links remained fixed. We found that the control is successful if the number of adapted links is equal to or higher than approximately 30% of all possible links, independently of the number of actual fixed links. For practical applications this opens up the possibility to apply the method more efficiently.

Given the paradigmatic nature of the Stuart-Landau oscillator as a generic model, we expect broad applicability, for instance, to control synchronization of networks in medicine, chemistry, or mechanical engineering or as self-organizing mechanisms in biological networks.

ACKNOWLEDGMENTS

This work was supported by Deutsche Forschungsgemeinschaft in the framework of SFB 910. J.L. acknowledges the support by the German-Russian Interdisciplinary Science Center (G-RISC) funded by the German Federal Foreign Office via the German Academic Exchange Service (DAAD). P.H. acknowledges support by the Federal Ministry of Education and Research (BMBF), Germany (Grant No. 01GQ1001B). We would like to thank Thomas Isele for fruitful discussion. A.S. and A.F. acknowledge support of RFBR (Grant No. 14-08-01015).

[1] S. Boccaletti, V. Latora, Y. Moreno, M. Chavez, and D. U. Hwang, Phys. Rep. **424**, 175 (2006).
[2] R. Albert and A. L. Barabasi, Rev. Mod. Phys. **74**, 47 (2002).
[3] M. E. J. Newman, SIAM Rev. **45**, 167 (2003).
[4] D. J. Watts and S. H. Strogatz, Nature (London) **393**, 440 (1998).
[5] A. Rapoport, Bull. Math. Biol. **19**, 257 (1957).
[6] P. Erdős and A. Rényi, Publ. Math. Debrecen **6**, 290 (1959).
[7] M. Dhamala, V. K. Jirsa, and M. Ding, Phys. Rev. Lett. **92**, 074104 (2004).
[8] M. Zigzag, M. Butkovski, A. Englert, W. Kinzel, and I. Kanter, Europhys. Lett. **85**, 60005 (2009).
[9] C. U. Choe, T. Dahms, P. Hövel, and E. Schöll, Phys. Rev. E **81**, 025205(R) (2010).
[10] M. Chavez, D. U. Hwang, A. Amann, H. G. E. Hentschel, and S. Boccaletti, Phys. Rev. Lett. **94**, 218701 (2005).
[11] F. Sorrentino and E. Ott, Phys. Rev. E **76**, 056114 (2007).
[12] R. Albert, H. Jeong, and A. L. Barabasi, Nature (London) **406**, 378 (2000).
[13] W. Kinzel, A. Englert, G. Reents, M. Zigzag, and I. Kanter, Phys. Rev. E **79**, 056207 (2009).
[14] J. Lehnert, T. Dahms, P. Hövel, and E. Schöll, Europhys. Lett. **96**, 60013 (2011).
[15] A. Keane, T. Dahms, J. Lehnert, S. A. Suryanarayana, P. Hövel, and E. Schöll, Eur. Phys. J. B **85**, 407 (2012).
[16] T. Gross and B. Blasius, J. R. Soc. Interface **5**, 259 (2008).
[17] T. Dahms, J. Lehnert, and E. Schöll, Phys. Rev. E **86**, 016202 (2012).
[18] I. Kanter, M. Zigzag, A. Englert, F. Geissler, and W. Kinzel, Europhys. Lett. **93**, 60003 (2011).
[19] I. Kanter, E. Kopelowitz, R. Vardi, M. Zigzag, W. Kinzel, M. Abeles, and D. Cohen, Europhys. Lett. **93**, 66001 (2011).
[20] M. Golubitsky and I. Stewart, *The Symmetry Perspective* (Birkhäuser, Basel, 2002).
[21] F. Sorrentino (unpublished).
[22] K. Blaha, J. Lehnert, A. Keane, T. Dahms, P. Hövel, E. Schöll, and J. L. Hudson, Phys. Rev. E **88**, 062915 (2013).
[23] C. R. S. Williams, T. E. Murphy, R. Roy, F. Sorrentino, T. Dahms, and E. Schöll, Phys. Rev. Lett. **110**, 064104 (2013).
[24] E. Mosekilde, Y. L. Maistrenko, and D. Postnov, *Chaotic Synchronization: Applications to Living Systems* (World Scientific, Singapore, 2002).

[25] A. Ijspeert, Neural Networks **21**, 642 (2008).
[26] B. Blasius, A. Huppert, and L. Stone, Nature (London) **399**, 354 (1999).
[27] X. Lu and B. Qin, Phys. Lett. A **373**, 3650 (2009).
[28] D. Hebb, *The Organization of Behavior: A Neuropsychological Theory*, new ed. (Wiley, New York, 1949).
[29] A. A. Selivanov, J. Lehnert, T. Dahms, P. Hövel, A. L. Fradkov, and E. Schöll, Phys. Rev. E **85**, 016201 (2012).
[30] A. L. Fradkov, *Cybernetical Physics: From Control of Chaos to Quantum Control* (Springer, Heidelberg, Germany, 2007).
[31] P. Erdős and A. Rényi, Publ. Math. Inst. Hung. Acad. Sci. **5**, 17 (1960).
[32] Y. Kuramoto, *Chemical Oscillations, Waves and Turbulence* (Springer-Verlag, Berlin, 1984).
[33] L. M. Pecora and T. L. Carroll, Phys. Rev. Lett. **80**, 2109 (1998).
[34] E. Schöll, A. A. Selivanov, J. Lehnert, T. Dahms, P. Hövel, and A. L. Fradkov, Int. J. Mod. Phys. B **26**, 1246007 (2012).
[35] A. L. Fradkov, Physics-Uspekhi **48**, 103 (2005).
[36] A. L. Fradkov and A. Y. Pogromsky, IEEE Trans. Circuits Syst. I, Fundam. Theory Appl. **43**, 907 (1996).